A Precise Gravity Tide Model for Port-au-Prince in Haiti

Olivier Francis[1], Kelly Guerrier[3] and Renaldo Sauveur[1,2,3]

[1] University of Luxembourg, Luxembourg
[2] Centre National de l'Information Géo-Spatiale, Haiti.
[3] URGéo-FDS-UEH, Haiti

Contact: Prof. Dr. O. Francis, Campus Belval, Maison du Nombre, 6, avenue de la Fonte, L-4364 Esch-sur-Alzette, Luxembourg.
Email : olivier.francis@uni.lu

January 2023

Introduction

In this report, we present the results of earth tides analyses of long gravity time series at two different locations in the city of Port-au-Prince in Haiti. Measurements from two different generations of relative spring gravimeters are used: the 20-year-old Scintrex CG5-008 of the University of Luxembourg and the new Scintrex CG6-270 from the "Unité de Recherche en Géosciences" (URGEO) of the Faculty of Sciences of the State University of Haiti. Technical details about the gravimeters can be found in the manuals of the Scintrex CG-5 (2012) and of the CG-6 Autograv (2019).

Continuous gravity observations were recorded by the Haitian authors of this report in their respective Institutes: the "Centre National de l'Information Géo-Spatiale" (CNIGS) and the URGEO. In addition to the gravity data, atmospheric pressure observations were collected. They are used to estimate the gravity attraction and loading effects due to the atmospheric pressure variations.

The earth tidal parameters are determined for both time series from the Scintrex CG5-008 and the Scintrex CG6-270. These parameters are extremely valuable either to assess the precision of the ocean tide models of the seas surrounding the Haitian Island or to make predictions of the gravity tides. Observed tidal parameters are indeed more precise than using a theoretical model of the Earth body tides combined with the attraction and loading gravity effects calculated with ocean tide models. These predictions provide the best tidal corrections for absolute gravity measurements as well as for relative gravity surveys on the Haitian Island. They will increase the accuracy of past and future geodetic observations.

After correcting the tidal parameters for the ocean loading and attraction effects calculated with a global ocean tides models, we found a close agreement with the state-of-the-art body earth model. On the other hand, the tidal parameters are sensitive to the structure and elastic properties of the upper crust (You and Yuan, 2021). The results presented in this report might be useful to investigate them.

At the time of this report, the data collection with the Scintrex CG5-008 was stopped while the Scintrex CG6-270 was still recording at the URGEO/BME site.

The report begins with a description of the gravity stations. We explain the data pre-processing applied to the raw measurements and show the "clean" time series. Those are the raw gravity observations edited for disturbances and small gaps being interpolated. They are then analyzed to extract the gravity tidal parameters. The estimated tidal parameters from the measurements are then compared with a body earth tides model including tidal oceanic loading and attraction effects. Finally, we discussed the results before concluding.

1. Description of the gravity stations

For the gravity stations, we selected two different sites in the city of Port-au-Prince (Figure 1). On the one hand, the Scintrex CG5-008 was installed on the main premises of the CNIGS close to the city center. On the other hand, the Scintrex CG6-270 from the URGEO was set up in a building of the "Bureau des Mines et de l'Energie" (BME) close to the international airport.

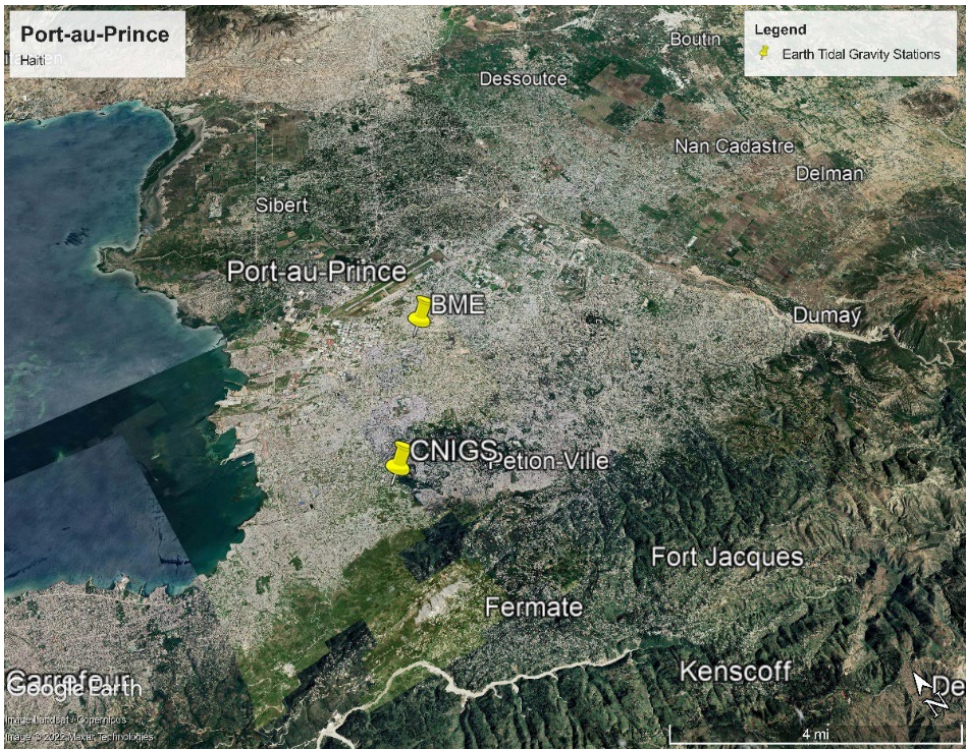

Figure 1. Sites used for continuous gravity measurements with the Scintrex CG5-008 at the "Centre National de l'Information Géo-Spatiale" (CNIGS) and the Scintrex CG6-270 at the site of the "Bureau des Mines et de l'Energie" (BME).

1.1 CNIGS site

From January 2018, the Scintrex CG5-008 operated for 10 months in one of the bungalows at the CNIGS (Figures 2). at 3.5 km from the sea in the south part of the city and close to its central area. The conditions were not ideal: the gravimeter was subjected to tilt perturbations due to the type of floor and disturbances caused by the proximity of the occupants of the office. Nonetheless, the room was equipped with air conditioning keeping the temperature relatively constant. The hourly atmospheric pressure observations were obtained from the "Unité Hydrométéorologique d'Haïti" (UHM) (meteo-haiti.gouv.ht) of the "Ministère de l'Agriculture des Ressources Naturelles et du Développement Rural" (MARNDR). The location coordinates are latitude 18.529560, longitude -72.323390 and altitude 127 m.

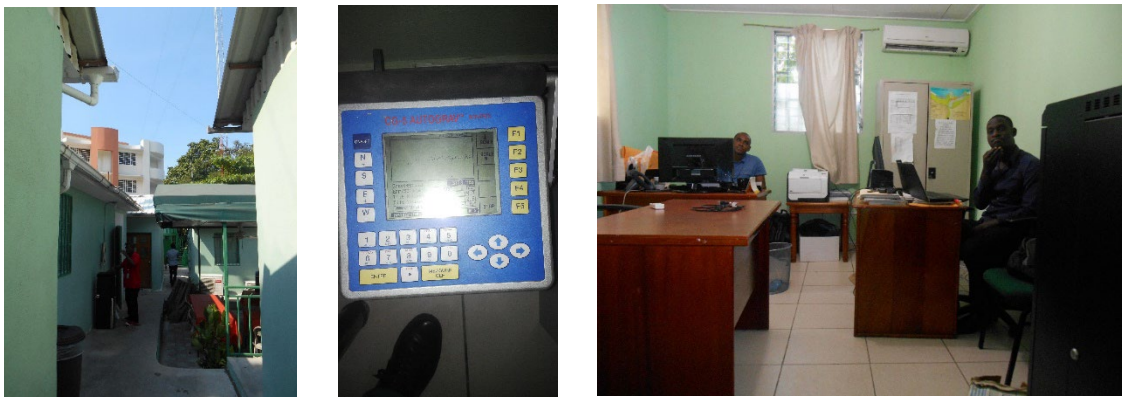

Figures 2. Some views of the site of the CINGS where the Scintrex CG5-008 performed continuous measurements for 10 months in 2018.

1.2 URGEO/BME site

The URGEO site is located in the northern part of Port-au-Prince. The Scintrex CG6-270 was installed in a building with a stable concrete floor without room temperature control. The occupancy of the office was very low due to the COVID-19 pandemic. The distance to the sea is 5.2 km. The distance to the CNIGS site is 4.5 km. The Scintrex CG6-270 is recording data continuously since the 10th of March 2021. One month later, a pressure sensor logger (Testo 176 P1, see references) started to record atmospheric pressure digital data with a time sampling of one data per minute. The location coordinates are latitude 18.562012, longitude -72.296232 and altitude 85 m.

Figures 3. Site for the "Bureau des Mines et de l'Energie" (BME) where the Scintrex CG6-270 is continuously recording gravity since 10-03-2021.

2. Data pre-processing and time series

For both Scintrex, we used the calibration factor provided by the manufacturer. All the pre-processing was performed using Tsoft (Van Camp and Vauterin, 2005). To clean the gravity observations, we proceed in the classical way using the remove-correct-restore method. First, the calibrated raw 1-min data are corrected for the gravity tides using a first guess prediction model. Secondly, the atmospheric pressure effect is removed by using the standard admittance factor of -3 nm s^{-2}/mbar. Then, the residuals are carefully edited: (1) the raw 1-min data are fixed for spikes, offsets, and all other non-tidal perturbations due to accidental tilts or earthquakes; (2) small gaps are also interpolated; and (3) the tidal prediction model and the atmospheric pressure correction are added back to the residuals to obtain clean time series. Finally, they are decimated to hourly observations by applying a symmetric low-pass filter with a cut-off period of 2 hour. The hourly gravity and atmospheric data are the inputs of the tides analysis software.

The Scintrex CG5-008 measured continuously for 285 days from 22-01-2018 to 03-11-2018 (Figures 4). We disregarded 93 days of data due to tilt disturbances that are not salvageable. A total of 192.5 days of data is kept that represents 67% of the raw data. We use a third-degree polynomial to eliminate most of the instrumental drift. The linear part of the drift is 101.3 nm s^{-2}/hour.

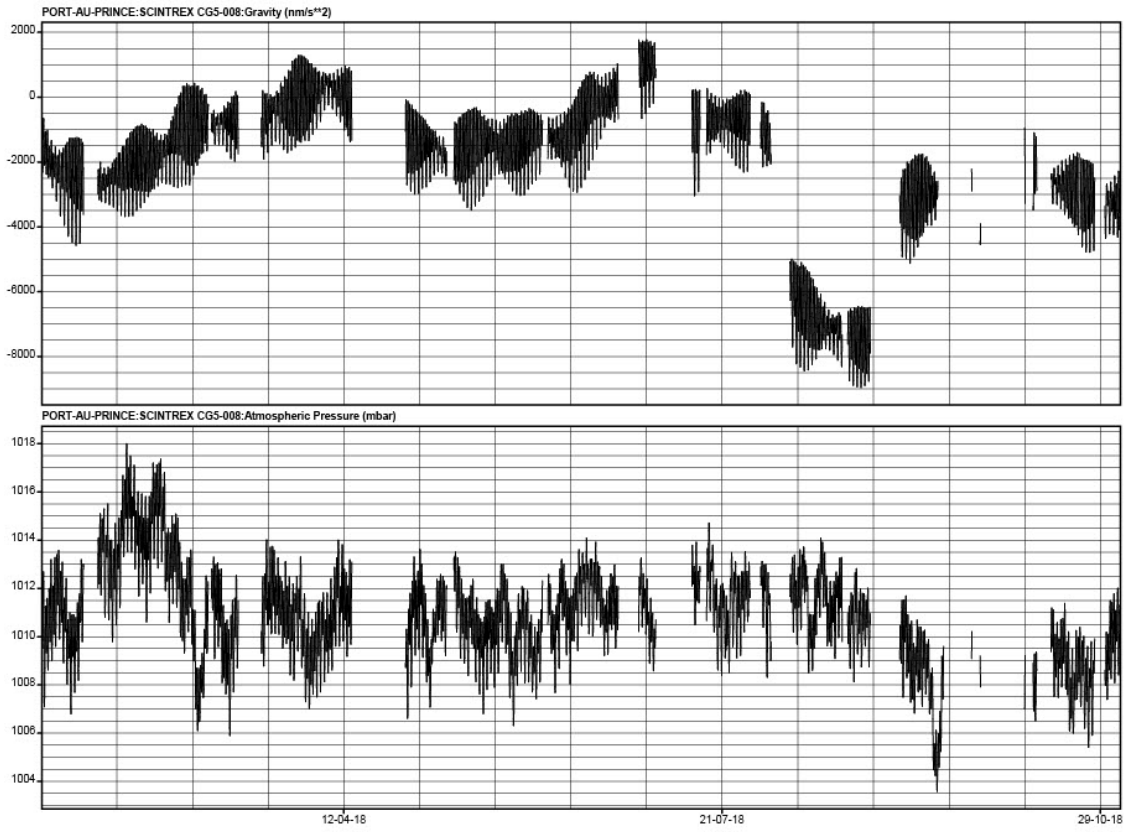

Figures 4. Edited hourly gravity data of the Scintrex CG5-008 and atmospheric pressure observations from the "Unité Hydrométéorologique d'Haïti" (UHM) in Port-au-Prince at the CNIGS from 22-01-2018 to 03-11-2018 (192.5 days). A third-degree polynomial is subtracted from the data to remove the long-term signal of the instrumental drift. The degree one (the linear part) is 101.3 nm s^{-2}/hour.

For the Scintrex CG6-270 (Figures 5), we considered 403.7 days of observations. The time series has two large data gaps due to accidental interruptions of either the gravimeter or the atmospheric logger acquisition systems.

After the first data gap, we observe an impressive change in the instrumental drift behaviour. At the beginning, the drift of the Scintrex CG6-270 is perfectly linear with a slope of -13.9 nm s^{-2}/hour. Its constant amplitude is 10 times smaller than the one of the Scintrex CG5-008 with an opposite sign. Then, the negative drift drastically increases before getting close to zero. After that tipping point, the drift becomes slightly positive and ends up as almost completely flat (i.e., zero drift). We have no explanation for this behaviour. No indications or evidence of external or internal parameters variation corroborate with the observed changes in the drift behaviour. At the end, we just look at the final low instrumental drift as a huge boon.

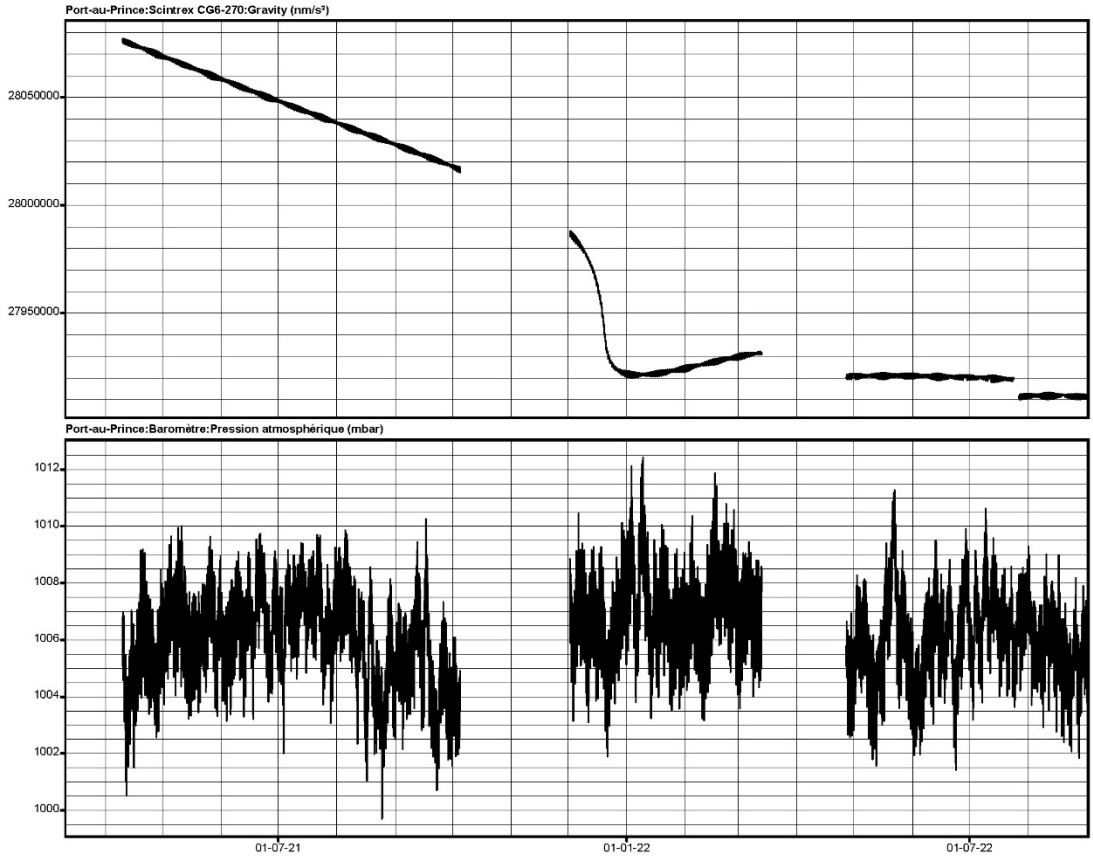

Figures 5. Edited hourly gravity data of the Scintrex CG6-270 and atmospheric pressure observations from a Testo 176 P1 logger at the Bureau des Mines et de l'Energie (BME/URGEO) in Port-au-Prince from 09-04-2021 to 01-09-2022 (403.7 days). We observe an initial linear drift of -13.9 nm s^{-2}/hour that almost vanishes towards the end of the time series.

3. Tidal analysis results

Earth tides analyses are performed with the Eterna software (Wenzel, 1996). The tidal parameters amplitude factors and phases (so-called delta factors and alpha) are jointly determined with the atmospheric admittance factor using the barometric pressure

records at the stations. These gravimetric delta factors and the alpha phase leads are estimated for specified tidal bands (or tidal waves). They are the transfer functions between the tidal potential and the gravity tides in well-chosen frequency bands around the larger tidal waves. In addition, the software can handle gaps in the data.

The number of tidal waves (related to the width of the tidal bands) that can be estimated increases with the length of the time series. Longer the time series are more tidal waves can be separated and estimated. For the Scintrex CG5-008, the half year of data allows us to estimate the tidal parameters for 15 waves. With more than a year of data, the Scintrex CG6-270 provides 36 tidal parameters. In general, the estimate of the quarter diurnal wave is unreliable because its amplitude is extremely small.

The results of the tidal analyses are presented in Tables 1 and 2 for the Scintrex CG5-008 and the Scintrex CG6-270, respectively. For the Scintrex CG6-270, the admittance factor for the atmospheric pressure presents a typical value close to the standard value of -3 nm s^{-2}/mbar. On the contrary for the Scintrex CG5-008, the value is definitively too high and questionable. The value is twice the standard value. The reasons could be a combination between the noise or/and the large gaps in the gravity observations as well as unknown issues with the atmospheric pressure data. Three aspects are affecting the Scintrex CG5's results: 1. Its measurements are less precise than those of the CG6 (Francis, 2021); 2. There are countless gaps in the time series, and; 3. The hourly atmospheric pressure data come from the UHM for which we have no information on the data precision. On the contrary for the Scintrex CG6-270, we used the data from our own meteorological sensor. The precision is about 0.1 mbar as its resolution.

Moreover, it is not surprising to obtain an unusual atmospheric pressure admittance factor for coastal stations especially on an island. Indeed, oceanic water responds as an inverted barometer that reduces considerably the loading effect on the ocean bottom. The latter has a positive admittance so the admittance for a coastal station will be more negative. This is what we observed in the results of the Scintrex CG5-008 but which is moderately confirmed by the results of the Scintrex CG6-270.

Overall, the results of the Scintrex CG6-270 are much more precise than those of the Scintrex CG5-008. It is mainly due to the instrumental improvements between the old generation versus the new generation of gravimeters. In addition, the Scintrex CG6-270 time series contains twice more data with far lesser gaps than the one of the Scintrex CG5-008. The site conditions also play a role: the Scintrex CG6-270 is set up on a more stable pillar and in a lesser visited site than the ones of the Scintrex CG5-008. However, the Scintrex CG6-270 is affected by the external temperature that explains the out-of-range delta factor for the S_1 tidal wave. Its value is 7 times larger than the value from the theoretical body tide model. This specific tidal constituent comprises also a radiational tide due the atmospheric thermal effect, which is larger than the gravitational S_1 tide. Obviously, the main origin of this anomaly is an instrumental thermal effect. Although the gravity data are corrected for internal temperature variations, it appears that the correction is not effective for a diurnal variation. It might be an indication that the temperature correction may be frequency dependent.

Unfortunately, we cannot separate the S_1 wave from the $P_1S_1K_1$ band for the Scintrex CG5-008 as the time series is not long enough. It seems less affected if we look at the K_1 tide result. The reason is that he Scintrex CG5-008 was installed in a room with air conditioning. Power Spectral Densities (PSDs) of the room temperatures and temperatures inside the gravimeters (not shown in this report) show a strong and dominant diurnal signal only for the Scintrex CG6-270.

Table 1. Earth gravity tidal parameters and atmospheric pressure admittance factor in Port-au-Prince at the CNIGS. They are estimated using 192.46 days of observations with the Scintrex CG5-008 from 22-01-2018 to 03-11-2018. Positive values of the "Phase Lead" mean that the gravity observations are in advance with respect to the tidal potential.

```
Program ETERNA, version 3.21 950117 Fortran 77
########################################################################
SCINTREX CG5-008
PORT AU PRINCE, HAITI
########################################################################
 Latitude: 18.5296 deg, longitude:-72.3236 deg, azimuth:  0.000 deg.

 Summary of observation data :
 20180122 30000...20180202 40000  20180205230000...20180307 40000
 20180308     0...20180315 20000  20180321 40000...20180414 30000
 20180428 70000...20180509 40000  20180511 20000...20180603120000
 20180604220000...20180611120000  20180611150000...20180623130000
 20180628220000...20180703100000  20180713     0...20180715 40000
 20180716210000...20180728100000  20180731 40000...20180802220000
 20180807220000...20180821180000  20180823 50000...20180829 40000
 20180905230000...20180916 10000  20180924230000...20180925 10000
 20180927 50000...20180927 80000  20181008230000...20181009 30000
 20181011 50000...20181012 40000  20181015230000...20181023100000
 20181023170000...20181027110000  20181030 50000...20181103 70000

 Initial epoch for tidal force    : 2018. 1.22. 0

 Number of recorded days in total :   192.46
 TAMURA 1987   tidal potential used.
 WAHR-DEHANT-ZSCHAU inelastic Earth model used.
 UNITY window used for least squares adjustment.
 Numerical filter is PERTSEV 1959 with  51 coefficients.

 Estimation of noise by FOURIER-spectrum of residuals
 0.1 cpd band99999.9990 nm/s**2       1.0 cpd band    1.7505 nm/s**2
 2.0 cpd band    0.8248 nm/s**2       3.0 cpd band    0.7759 nm/s**2
 4.0 cpd band    0.5461 nm/s**2       white  noise    0.7557 nm/s**2

 Adjusted tidal parameters :
 from      to      wave   ampl. ampl.fac.    stdv. ph. lead    stdv.
 [cpd]     [cpd]     [nm/s**2 ]                        [deg]    [deg]
 0.721500 0.906315 Q1    41.204   1.15131  0.02932  -0.5665   1.6781
 0.921941 0.940487 O1   220.007   1.17699  0.00562   1.4832   0.3193
 0.958085 0.974188 M1    15.544   1.05735  0.07656  11.0225   4.3164
 0.989049 0.998028 P1   101.792   1.17037  0.01079   2.6769   0.6526
 0.999853 1.011099 K1   305.664   1.16271  0.00419   2.0599   0.2217
 1.013689 1.044800 J1    17.494   1.19000  0.07552   2.1517   4.2657
 1.064841 1.216397 OO1   10.526   1.30897  0.17634  30.4115  10.1319
 1.719381 1.872142 2N2   24.534   1.18968  0.01628  -0.3342   0.9336
 1.888387 1.906462 N2   152.206   1.17864  0.00327   0.4203   0.1868
 1.923766 1.942754 M2   797.744   1.18274  0.00064   0.3195   0.0363
 1.958233 1.976926 L2    22.482   1.17926  0.02331  -1.5570   1.3329
 1.991787 2.002885 S2   370.828   1.18171  0.00143  -0.7882   0.1433
 2.003032 2.182843 K2   100.014   1.17269  0.00615  -0.5156   0.3527
 2.753244 3.081254 M3    12.596   1.00227  0.02887   1.3507   1.6550
 3.791964 3.937897 M4     0.839   3.86894  1.13735  33.0037  65.1824

 Adjusted meteorological or hydrological parameters:
 no. regr.coeff.       stdv.  parameter   unit
   1    -6.73509     0.52570  air press.  nm/s**2 /

 Standard deviation of weight unit:    16.800
 degree of freedom:                     3652
 Standard deviation:                   16.800  nm/s**2
```

Table 2. Earth gravity tidal parameters and atmospheric pressure admittance factor in Port-au-Prince at the URGEO/BME. They are estimated using 403.67 days of observations with the Scintrex CG6-270 from 09-04-2021 to 01-09-2022. Positive values of the "Phase Lead" mean that the gravity observations are in advance with respect to the tidal potential.

```
Program ETERNA, version 3.21 950117 Fortran 77
########################################################################
SCINTREX CG6-270
PORT-AU-PRINCE, HAITI
########################################################################
 Latitude: 18.5620 deg, longitude:-72.2962 deg, azimuth:  0.000 deg.

 Summary of observation data :
 20210409230000...20211005 50000  20211202 30000...20220313 60000
 20220427     0...20220430 50000  20220430220000...20220724 70000
 20220727 20000...20220901140000

 Initial epoch for tidal force    : 2021. 4. 9. 0

 Number of recorded days in total :   403.67
 TAMURA 1987   tidal potential used.
 WAHR-DEHANT-ZSCHAU inelastic Earth model used.
 UNITY window used for least squares adjustment.
 Numerical filter is PERTSEV 1959 with  51 coefficients.

 Estimation of noise by FOURIER-spectrum of residuals
 0.1 cpd band99999.9990 nm/s**2       1.0 cpd band    0.7594 nm/s**2
 2.0 cpd band    0.3840 nm/s**2       3.0 cpd band    0.3089 nm/s**2
 4.0 cpd band    0.2369 nm/s**2       white  noise    0.3147 nm/s**2

 adjusted tidal parameters :
 from      to      wave   ampl. ampl.fac.    stdv. ph. lead    stdv.
 [cpd]     [cpd]     [nm/s**2 ]                        [deg]    [deg]
 0.721499 0.833113 SGQ1   2.143   1.54983  0.24937   8.7683  14.2854
 0.851182 0.859691 2Q1    6.009   1.26701  0.08583   4.1422   4.9258
 0.860896 0.870023 SGM1   6.007   1.04945  0.07435   3.9753   4.2595
 0.887325 0.896130 Q1    42.992   1.19947  0.01123   1.8594   0.6453
 0.897806 0.906315 RO1    7.963   1.16960  0.05931  -1.7751   3.3977
 0.921941 0.930449 O1   222.719   1.18972  0.00211   1.2421   0.1209
 0.931964 0.940488 TAU1   2.583   1.05792  0.22548  -6.0396  12.9164
 0.958085 0.966756 NO1   18.153   1.23297  0.03591  -0.6662   2.0490
 0.968565 0.974189 CHI1   3.717   1.32014  0.14043   1.1377   8.0583
 0.989048 0.995144 PI1    7.587   1.49039  0.10370 -22.2959   5.9413
 0.996967 0.998028 P1   105.605   1.21239  0.00624   0.7225   0.3601
 0.999852 1.000148 S1    14.900   7.23937  0.52764-139.4243  31.9181
 1.001824 1.003651 K1   307.536   1.16808  0.00211   1.1595   0.1199
 1.005328 1.005623 PSI1   1.056   0.51301  0.25678  16.7195  14.7181
 1.007594 1.013689 PHI1   6.671   1.77992  0.15093  -8.1177   8.6303
 1.028549 1.034467 TET1   3.502   1.24407  0.14736   2.7012   8.4473
 1.036291 1.044800 J1    17.863   1.21330  0.02567   1.2815   1.4722
 1.064841 1.071083 SO1    3.530   1.44554  0.16566   3.7365   9.4952
 1.072583 1.080945 OO1    9.385   1.16540  0.04342   0.8782   2.4844
 1.099161 1.216397 NU1    1.475   0.95642  0.20588  -9.2559  11.7910
 1.719380 1.837970 EPS2   5.571   1.11852  0.04117  -0.2485   2.3584
 1.853920 1.862429 2N2   20.172   1.18088  0.01473  -0.7971   0.8444
 1.863634 1.872142 MU2   23.874   1.15809  0.01161   1.4870   0.6650
 1.888387 1.896748 N2   152.830   1.18390  0.00184   0.5541   0.1053
 1.897954 1.906462 NU2   28.829   1.17577  0.00945   0.6676   0.5412
 1.923765 1.942754 M2   798.203   1.18385  0.00032   0.3576   0.0184
 1.958232 1.963709 LAM2   5.548   1.11580  0.04636   2.3235   2.6562
 1.965827 1.976926 L2    22.672   1.18966  0.00801  -0.1117   0.4589
 1.991786 1.998288 T2    20.910   1.14086  0.01286   1.1725   0.7753
 1.999705 2.000766 S2   370.625   1.18149  0.00090   0.1063   0.1064
 2.002590 2.013689 K2   100.242   1.17583  0.00235  -0.0150   0.1352
 2.031287 2.047390 ETA2   5.416   1.13616  0.03707   0.5657   2.1237
 2.067579 2.182844 2K2    1.416   1.13410  0.12097  -1.0789   6.9274
 2.753243 2.869714 MN3    3.904   1.13274  0.04954  -2.3094   2.8372
```

```
2.892640 3.081254 M3    13.489   1.07385  0.01346   0.1955   0.7716
3.791963 3.901458 M4     0.334   1.54190  0.57391  38.9295  32.8810

Adjusted meteorological or hydrological parameters:
no. regr.coeff.       stdv.  parameter   unit
  1    -3.57597     0.36969              nm/s**2 /

Standard deviation of weight unit:    11.912
degree of freedom:                     9365
Standard deviation:                   11.912  nm/s**2
```

4. Comparison with tidal oceanic loading and attraction

For each tidal wave, we calculate the inelastic non-hydrostatic body tide Earth response **R**(R,0) with the theoretical model of Dehant et al (1999) that we compare with the observed tidal response **A**(A,α) (see Figure 6). The vector **B**(B,β) is formed by taking their vector difference, which mostly contains the tidal oceanic loading and attraction. By removing the oceanic loading and attraction vector calculated with a global ocean tides model, we obtain the final residue vector **X**(X,χ).

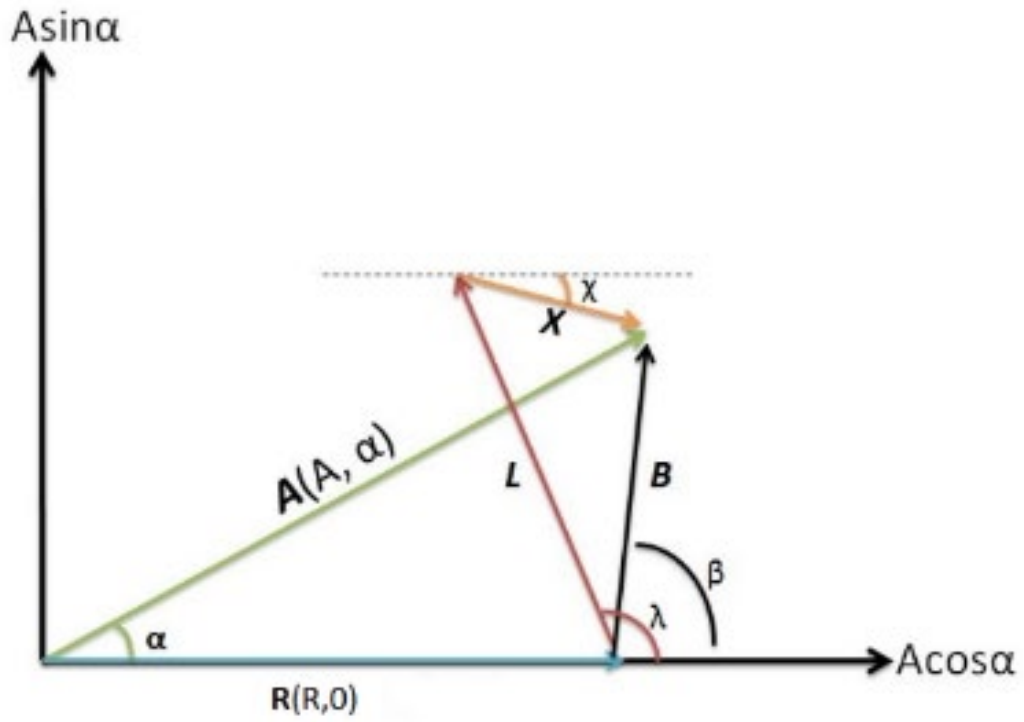

Figure 6. Vector diagram: **A**(A, α) is the observed tidal response; **R**(R,0) inelastic non-hydrostatic ocean-less Earth model response (Dehant et al., 1999); **B**(B, β) = **A**-**R;** **L**(L,λ) oceanic attraction and loading vector (calculated with an ocean tides model); **X**(X,χ) = **B** – **L** = **A** – **R** – **L** is the final residue vector.

The amplitude X of the residue vectors should be around a few nm s^{-2} (see Ducarme 2009, for example) when the observations are good and if the ocean tides model provides with a good estimate of the ocean loading and attraction effects. The X is a measure of the quality of the tidal analysis results and subsequently of the gravity tides prediction based on the observed tides. We used the FES2004 ocean tides model (Lyard

et al., 2006) which gives the best results on average when considering the main diurnal (Q_1, O_1, P_1, K_1) and semi-diurnal tidal (N_2, M_2, S_2, K_2) waves.

In table 3, we see a good match between the observed gravity tides corrected for the ocean tide loading using the FES2004 model and the theoretical inelastic non-hydrostatic body tides model of Dehant et al. (1999) The residue vectors are relatively small with amplitudes less than 5 nm s^{-2} with one exception for K_1 obtained with the Scintrex CG5-008. Overall, the amplitudes of the residue vectors are smaller for the Scintrex CG6-270 except for N_2 and M_2 although very close to the results of the Scintrex CG5-008. We can conclude that the results of the tidal analyses are good for the Scintrex CG5-008 and excellent for the Scintrex CG6-270.

Table 3. **A**(A,α) is the observed tidal response; **R** (R,0) elastic ocean-less Earth model response (Dehant et al., 1999); **B**(B, β) = **A**-**R; L**(L,λ) oceanic attraction and loading vector (calculated with the FES2004 global ocean tides model, Lyard et al., 2006); **X**(X,χ) = **B** – **L** = **A** – **R** – **L** is the final residue vector.

Wave	**A** /nm s^{-2}	α degree	**R** /nm s^{-2}	**B** /nm s^{-2}	β degree	**L** /nm s^{-2}	λ Degree	**X** /nm s^{-2}	χ degree
				Scintrex CG5-008					
Q_1	41.2	-0.6	35.8	0.4	255.8	1.6	56.1	2.0	240.1
O_1	220.0	1.5	186.9	7.1	53.6	7.7	34.6	2.5	148.9
P_1	101.8	2.7	87.0	5.1	70.1	3.1	31.2	3.3	106.1
K_1	305.7	2.1	262.9	13.0	57.8	9.4	30.8	6.3	100.3
N_2	152.2	0.4	129.1	2.5	27.1	2.6	35.7	0.4	280.3
M_2	797.7	0.3	674.5	14.9	17.4	14.6	13.4	1.1	91.1
S_2	370.8	-0.8	313.8	8.1	320.8	5.6	350.4	4.2	279.9
K_2	100.0	-0.5	85.3	1.3	316.1	1.6	352.0	0.9	227.7
				Scintrex CG6-270					
Q_1	43.0	1.9	35.8	2.1	41.0	1.6	56.3	0.7	4.5
O_1	222.7	1.2	187.2	8.2	36.1	7.7	34.7	0.5	58.2
P_1	105.6	0.7	87.1	5.6	13.6	3.1	31.4	2.9	-5.2
K_1	307.5	1.2	263.3	10.5	36.3	9.3	31.0	1.5	71.0
N_2	152.8	0.6	129.1	3.2	27.3	2.6	35.3	0.7	-3.4
M_2	798.2	0.4	674.2	15.7	18.5	14.7	13.1	1.8	69.6
S_2	370.6	0.1	313.7	6.2	6.3	5.6	350.3	1.8	66.8
K_2	100.2	-0.0	85.3	1.2	-1.2	1.6	351.9	0.4	150.8

5. Discussion

In Figures 7 and 8, the observed delta factors and phase leads for the main diurnal and semi-diurnal tidal waves are displayed in red for both Scintrex. In the same figures, the delta factors and phases corrected for the ocean loading and attraction effects using the FES2004 (Lyard et al., 2006) ocean tides model are displayed in blue.

We used four different ocean tides models to calculate the loading and attraction effects: Schwiderski (1980), CSR3.0 (Eanes and Bettadpur, 1995), FES952 and FES2004 (Lyard et al., 2006). The three last models give similar results. This is the reason why we present the results only for the FES2004 that is the best model in average. It is interesting to note that none of the global ocean tides models provide a fully satisfactory agreement with the theoretical values. However, the agreement between the observed and theoretical tidal factors always improves with the ocean loading and attraction corrections whatever ocean tide model is used.

In the semi-diurnal band, the match with the theoretical model (Dehant et al., 1999) is similar for both gravimeters. For the N_2 tide, the delta factor from the Scintrex CG5-008 perfectly fit the model while the phase from the Scintrex CG6-270 is also a perfect fit with the model.

In the diurnal band, the amplitudes of the delta factors of the Scintrex CG5-008 are systematically too low with large phase differences except for O_1. The latter is in perfect agreement in amplitude as well in phase with the theoretical model. All the phases from the Scintrex CG6-270 match the model very closely. Only, the P_1 delta factor for the Scintrex CG6-270 is further away from the model. Despite that, the final residue is smaller for the Scintrex CG6-270 (see Table 3) because its phase is in perfect agreement with the theoretical model which is not the case for the Scintrex CG5-008.

The observed tidal parameters could be useful to test more global ocean tides models in that region. In fact, it would be worth to supplement global ocean tides models with local and regional ocean tides maps to improve the ocean loading and attraction corrections.

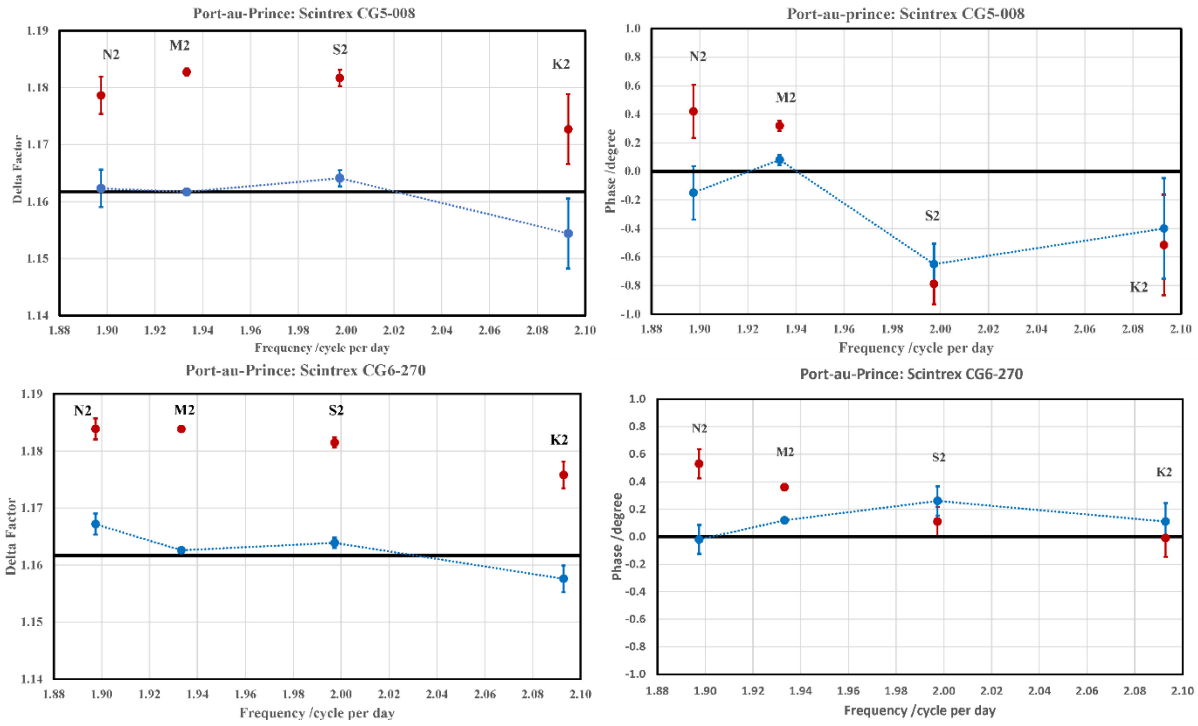

Figures 7. Observed semi-diurnal tidal parameters in Port-au-Prince estimated from the analyses of the time series of the Scintrex CG5-008 and CG6-270. The red dots are the observed delta factors and phases. The blue dots connected by a line are the delta factors and phases after correcting for the ocean loading and attraction using the FES2004 oceanic tides model. The black lines represent the Dehant et al. (1999) Earth tide model.

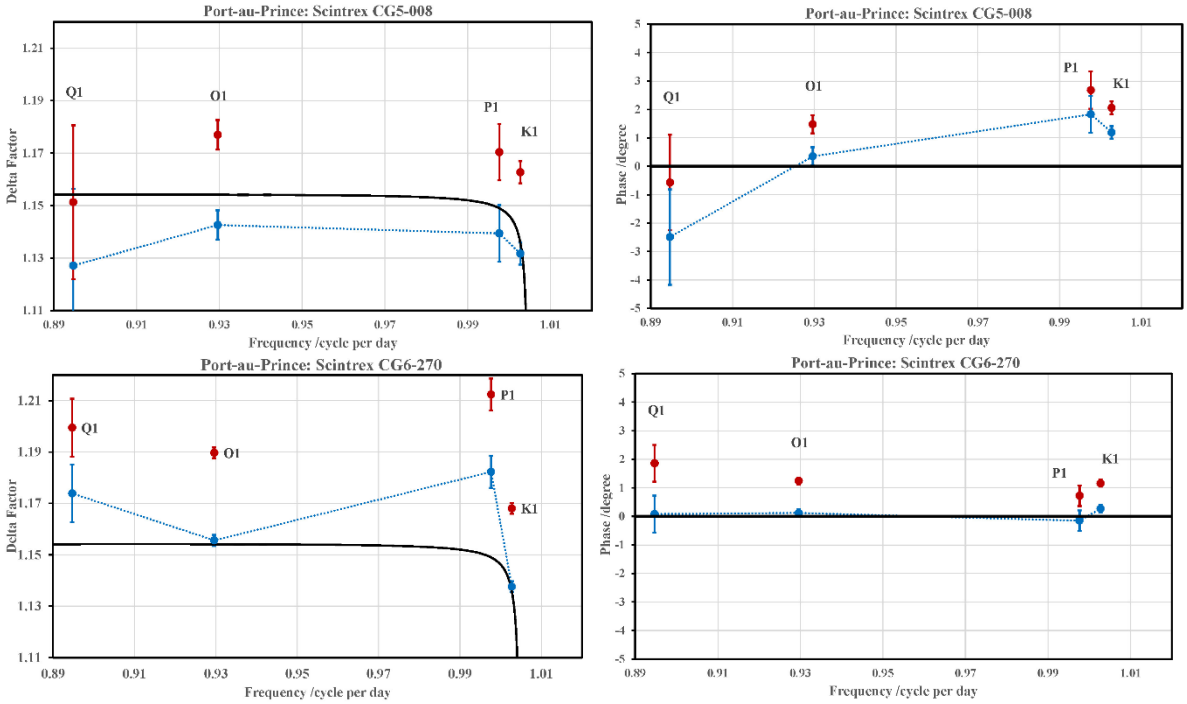

Figures 8. Observed diurnal tidal parameters in Port-au-Prince estimated from the analyses of the time series of the Scintrex CG5-008 and CG6-270. The red dots are the observed delta factors and phases. The blue dots connected by a line are the delta factors and phases after correcting for the ocean loading and attraction using the FES2004 oceanic tides model. The black lines represent the Dehant et al. (1999) Earth tide model.

6. Conclusions

Observed gravity tidal parameters are obtained with two relative gravimeters (Scintrex CG5-008 and CG6-270) at two different locations in Port-au-Prince in Haiti. The Scintrex CG6-270 provides the best results for different reasons: the CG6 being an improved version of the CG5 is more precise, the times series of the CG6 is twice longer than the CG5's one and, the CG6 was operating on a more stable floor.

The amplitude factor of the S_1 tide for the Scintrex CG6-003 is out of range. It is correlated with the external temperature that has an amplitude of 2 degree Celsius also at the S_1 tide. For gravity tide prediction, we can ignore the constituent S_1 or simply use the theoretical amplitude of 1.14618. This thermal effect is not visible in the Scintrex CG5-008 data because the gravimeter operated in a temperature-controlled environment with air conditioning.

Gravity tidal parameters are now available to make highly precise predictions of the gravity tides in and around Port-au-Prince in Haiti.

References

Dehant V., Defraigne P. and Wahr J.M., Tides for a convective Earth, J. Geophys. Res., 104, B1, pp. 1035-1058, 1999.

Ducarme, B., Limitations of High Precision Tidal Prediction, Bulletin d'Information des Marées Terrestres, 145, 11663-11677, 2009.

Eanes R.J. and S. Bettadpur, The CSR 3.0 global ocean tide model, Technical Memorandum CSR-TM-95-06, Center for Space Research, University of Texas, Austin, Tx. 1995.

Francis, O., Performance assessment of the relative gravimeter Scintrex CG-6. *J Geod* **95**, 116 (2012). https://doi.org/10.1007/s00190-021-01572-y

Lyard F., F. Lefevre, T. Letellier and O. Francis, Modelling the global ocean tides: modern insights from FES2004, Ocean Dynamics, DOI 10.1007/s10236-006-0086-x, 2006.

Melchior P., The Tides of the Planet Earth, Oxford, Pergamon, 1983.

Scintrex Ltd (2021) CG-5 scintrex autograv system operation manual, part 1 # 867700 revision 8, Scintrex Limited, Concord.

Scintrex Ltd (2019) CG-6 operations manuals RevC, https://scintrexltd.com/wp-content/uploads/2019/03/CG-6-Operations-Manual-RevC.pdf/

Schwiderski, E, .W, On charting global ocean tides, Reviews of Geophysics and Space Physics,18, 243-268, 1980.

Testo 176 P1, https://www.testo.com/fr-FR/enregistreur-de-temperature-humidite-pression-testo-176-p1/p/0572-1767

Van Camp, M., and Vauterin, P., Tsoft: graphical and interactive software for the analysis of time series and Earth tides, Computers in Geosciences, 31(5) 631-640, 2005.

Wenzel, H-G., The nanogal software: Earth tide data processing package: ETERNA 3.3, Bulletin d'Information des Marées Terrestres, 124, 9425-9439, 1996.

You, X., Yuan, L., The sensitivity of ocean tide loading displacements to the structure of the upper mantle and crust of Taiwan Island. *Earth Planets Space* **73**, 193 (2021). https://doi.org/10.1186/s40623-021-01525-x